THE JOURNAL OF PHYSICAL CHEMISTRY B

Article

pubs.acs.org/JPCB

A Map of Dielectric Heterogeneity in a Membrane Protein: the Hetero-Oligomeric Cytochrome b_6f Complex

S. Saif Hasan,[†,∥] Stanislav D. Zakharov,[†,§,∥] Adrien Chauvet,[‡] Valentyn Stadnytskyi,[‡] Sergei Savikhin,*[,‡] and William A. Cramer*[,†]

[†]Department of Biological Sciences and [‡]Department of Physics, Purdue University, West Lafayette, Indiana 47907, United States

[§]Institute of Basic Problems of Biology, Russian Academy of Science, Pushchino, Moscow Region 142290, Russian Federation

Supporting Information

ABSTRACT: The cytochrome b_6f complex, a member of the cytochrome bc family that mediates energy transduction in photosynthetic and respiratory membranes, is a hetero-oligomeric complex that utilizes two pairs of b-hemes in a symmetric dimer to accomplish trans-membrane electron transfer, quinone oxidation−reduction, and generation of a proton electrochemical potential. Analysis of electron storage in this pathway, utilizing simultaneous measurement of heme reduction, and of circular dichroism (CD) spectra, to assay heme−heme interactions, implies a heterogeneous distribution of the dielectric constants that mediate electrostatic interactions between the four hemes in the complex. Crystallographic information was used to determine the identity of the interacting hemes. The Soret band CD signal is dominated by excitonic interaction between the intramonomer b-hemes, b_n and b_p, on the electrochemically negative and positive sides of the complex. Kinetic data imply that the most probable pathway for transfer of the two electrons needed for quinone oxidation−reduction utilizes this intramonomer heme pair, contradicting the expectation based on heme redox potentials and thermodynamics, that the two higher potential hemes b_n on different monomers would be preferentially reduced. Energetically preferred intramonomer electron storage of electrons on the intramonomer b-hemes is found to require heterogeneity of interheme dielectric constants. Relative to the medium separating the two higher potential hemes b_n, a relatively large dielectric constant must exist between the intramonomer b-hemes, allowing a smaller electrostatic repulsion between the reduced hemes. Heterogeneity of dielectric constants is an additional structure−function parameter of membrane protein complexes.

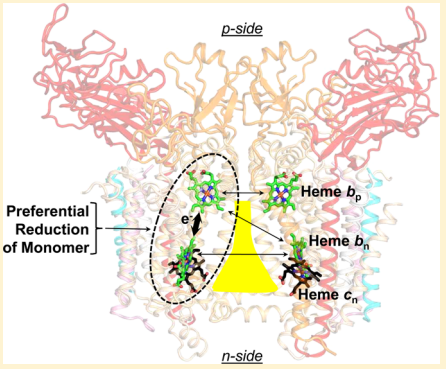

1. INTRODUCTION

Photosynthetic and respiratory electron transfer chains utilize a series of membrane bound multisubunit protein complexes.[1−4] Recent advances in membrane protein structural biology have described static structure-related aspects of such large membrane protein assemblies. An exponential increase in the number of membrane protein structures solved to high resolution (http://blanco.biomol.uci.edu/mpstruc/),[5] including hetero-oligomeric electron transfer complexes, has enhanced the understanding of the protein architecture and the intraprotein environment of the associated prosthetic groups. An important feature of the multisubunit membrane protein complexes involved in electron transfer is the presence of ordered, crystallographically resolvable lipids and lipid binding sites,[6−8] and the presence of cavities lined by hydrophobic residues within the trans-membrane domain proposed to provide conduits for binding and transport of redox substrates, such as quinones.[6,8−13] The redox prosthetic groups of membrane protein electron transfer complexes are mostly embedded in the trans-membrane domain. Domains of these complexes that contain an extended lipid matrix are assumed to have a low dielectric constant, approximately 2.5.[14−16]

Investigation of the effects of dielectric heterogeneity in membrane protein function requires a system with unique measurable signals across a medium with different dielectric constants. The cytochrome b_6f complex is a dimeric lipoprotein integral membrane complex that catalyzes plastoquinone reduction−protonation at the electrochemically negative (n) side of the thylakoid membrane and plastoquinol deprotonation−oxidation on the electrochemically positive (p) side.[11,17] The trans-membrane core of the dimeric cytochrome b_6f complex is associated with four b-hemes with separable redox potentials between two of lower potential (b_L or b_p) and two of higher potential (b_H or b_n).[18−20] The heme b_p/b_n pair is embedded in a protein environment, within the monomeric unit of the b_6f complex, while the two monomers are separated by a large cavity (30 Å high, 15 Å deep, 25 Å wide on the n-side), which is known to contain an appreciable lipid content.[21] The presence of an intramembrane, asymmetrically located lipid-filled cavity in such a membrane protein complex is expected to contribute significantly to the energetics of electron

Received: February 3, 2014
Revised: April 29, 2014
Published: May 27, 2014

   dx.doi.org/10.1021/jp501165k | J. Phys. Chem. B 2014, 118, 6614−6625

transfer reactions, and perhaps to contribute to a heterogeneous distribution of dielectric constants within the complex.

The structure of the hetero-oligomeric lipoprotein cytochrome b_6f complex, which couples proton translocation and electron transport in oxygenic photosynthesis, has been obtained from two filamentous cyanobacteria, *Mastigocladus laminosus* (Figure 1A) and *Nostoc* sp. PCC 7120,[11−13,22,23] and

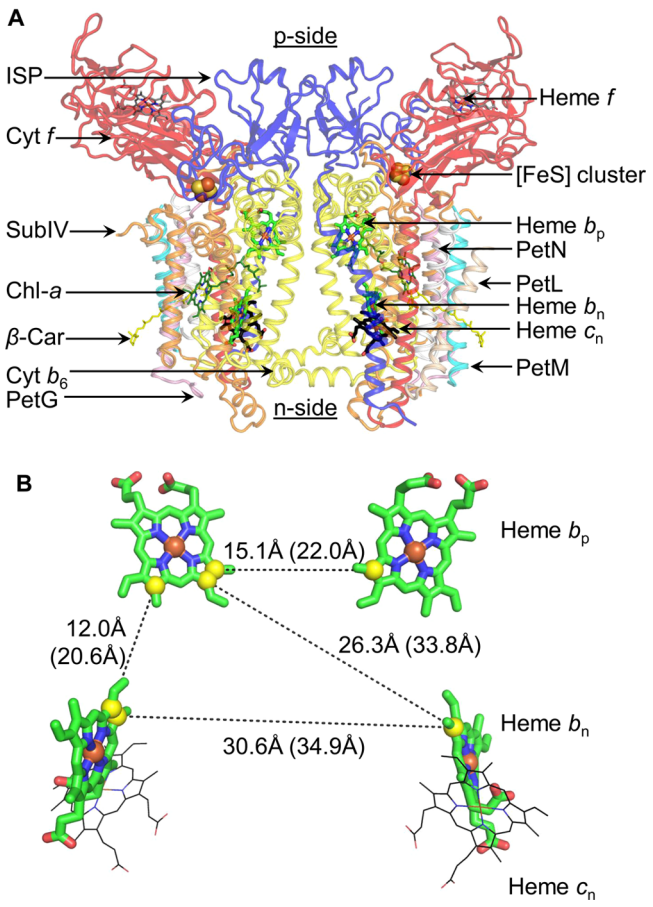

Figure 1. (A) Cytochrome b_6f complex structure from *Nostoc* PCC 7120 (PDB ID 4H44). Ribbon diagram of polypeptide subunits and redox active groups. Cytochrome b_6 subunit, yellow; subunitIV, orange; cytochrome *f*, red; Rieske [2Fe−2S] iron−sulfur protein, blue; PetG, pink; PetL, wheat; PetM, cyan; PetN, white. Hemes b_p and b_n (green, red, and blue), c_n (black, red, and blue), *f* (gray, red, and blue), chlorophyll-*a* (dark green and blue), and *β*-carotene (yellow) are shown as sticks. The components of the [2Fe−2S] cluster of the Rieske iron−sulfur protein are depicted as spheres (Fe, brown; sulfur, yellow). (B) Geometry of hemes within the trans-membrane domain of cytochrome b_6f (PDB 4H44). Edge−edge and center−center (Fe−Fe, in parentheses) distances are shown.

the green alga, *Chlamydomonas reinhardtii*.[24] The hydrophobic core of the b_6f complex is similar[21] to the core of the related cytochrome bc_1 complex in the mitochondrial respiratory chain and purple photosynthetic bacteria.[6,9,25−27] In this core, the two trans-membrane *b*-hemes, b_n and b_p, respectively, on the n- and p-sides of the complex, cross-link the "B" and "D" TMH of the cytochrome *b* subunit through *bis*-histidine ligation in each monomer of a symmetric dimer,[28] a structure motif also present in the cytochrome bc_1 complex.[9,25,28] The b_6f complex accepts electrons from plastoquinol, transfers one electron to the plastocyanin or cytochrome c_6 of higher oxidation−reduction potential on the p-side of the complex, and can transfer the other to a lower potential trans-membrane pathway involving the two *b*-hemes b_p and b_n directed to a plastoquinone bound axially to the heme c_n.[11,13] The electron transfer reactions are coupled to net proton transfer, whose pathways have been described,[11] into the aqueous phase on the p-side of the membrane, thereby contributing to the trans-membrane electrochemical proton gradient utilized for ATP synthesis. A summary of the net electron and proton transfer pathways is shown (Figure S1, Supporting Information) along with edge−edge and center−center distances between the trans-membrane *b*-hemes in the b_6f complex (Figure 1B) and heme center (Fe)−center (Fe) distances (Figure 1B, Table 1).

Table 1. Relative Contribution of *b*-Heme Pairs to the CD Signal in the Dimeric Cytochrome b_6f Complex[a]

heme pair[b]	center−center distance (Å)	interplanar angle (deg)	relative contribution to CD spectrum (%)
b_{p1}−b_{n1}	20.6	52.0	+50.8%
b_{p2}−b_{n2}			+50.8%
b_{p1}−b_{p2}	22.0	17.2	−3.5%
b_{p1}−b_{n2}	33.8	48.4	+3.2%
b_{p2}−b_{n1}			+3.2%
b_{n1}−b_{n2}	34.9	18.9	−4.5%

[a]Center-to-center distances, interplanar angles, and calculation of relative CD amplitudes determined from the crystal structure (PDB ID 4H44). [b]Additional numerical subscripts in *b*-heme notation used to distinguish the hemes in the two monomers of the dimeric complex.

The cytochrome b_6f complex, its structure determined from crystallographic analysis shown in ribbon format (Figure 1A), contains five redox prosthetic groups: the extra-membrane heme of cytochrome *f*; the two trans-membrane *b*-hemes; heme c_n, which is electronically coupled to heme b_n;[29,30] and the [2Fe−2S] cluster in the iron−sulfur protein subunit at the p-side membrane interface. The edge−edge distances between the trans-membrane *b*-hemes, which are a major determinant of the rate of intraprotein electron transfer,[31−35] are, respectively, 8.1 and 12.8 Å (Figure 1B), between the intramonomer *b*-hemes, b_p and b_n, and the intermonomer hemes, b_p, as seen in the crystal structure of the *Nostoc* PCC 7120 cytochrome b_6f complex (PDB ID 4H44).[11] Heme center−center distances, one determinant of the strength of interheme exciton interactions, are shown in Figure 1B and summarized (Table 1).

In addition to conferring structure stability, an obligatory function in electron transfer of the dimeric structure of the cytochrome b_6f complex has not been described, and little is known about the physical interactions that govern the pathways of trans-membrane electron transfer between bound quinone molecules on the two sides of the membrane via the two *b*-type hemes. The electron transfer pathways in cytochrome *bc* complexes have been studied extensively in the respiratory and photosynthetic bacterial cytochrome bc_1 complex,[36−44] for which crystal structure information has been summarized.[21,45,46] It was inferred from the absence of a sigmoidal dependence of flash-induced cytochrome *b* reduction in the presence of the inhibitor myxathiazol,[38] and the shorter distance between the intramonomer hemes b_p and b_n compared to the distances between the intermonomer *b*-hemes,[42] that intramonomer electron transfer from heme b_p to heme b_n is more likely than intermonomer transfer between the two hemes b_p. A different viewpoint is that interheme transfer

dx.doi.org/10.1021/jp501165k | J. Phys. Chem. B 2014, 118, 6614−6625

between hemes b_p in the two monomers can occur with comparable likelihood,[36,41,43,47] described as "half sites reactivity",[37,44] and proposed[48] in the context of the first crystal structures of the mitochondrial bc_1 complex. Efficient communication between the two monomers at the level of the *b*-hemes was demonstrated through mutagenesis of the bc_1 complex in the photosynthetic bacteria, *Rhodobacter capsulatus*[39,41,43] and *Rb. sphaeroides*.[49] The issue in the latter studies is the pathway preferred for transfer of a single electron. The present study concerns the most probable pathway for transfer of the pair of electrons required for the complete two-electron reduction of the quinone bound on the n-side of the cytochrome *bc* complex.

While low temperature spectra distinguish hemes b_p and b_n, the pathway of electrons through the b_6f dimer cannot be determined, as the spectra of the two hemes b_p (or b_n) in the dimer cannot be distinguished in kinetic studies at room temperature.[50] However, the asymmetric arrangement of the *b*-hemes within the b_6f dimer results in unique interactions between various *b*-heme pairs. The existence of physical interactions between the *b*-hemes involved in trans-membrane electron transfer in mitochondrial and chloroplast membranes has previously been inferred from excitonic circular dichroism (CD) spectra of dithionite-reduced isolated cytochrome bc_1[51] and b_6f[52] complexes. In the Soret band region, the CD spectra of dithionite-reduced cytochrome bc_1 and b_6f complex are split, due to excitonic heme−heme interactions, into two lobes of opposite sign around a node near the Soret band absorbance peak (432 nm). The amplitude of the split CD spectrum is a function of the geometry (interheme angle and distance) of the interacting hemes. High resolution crystal structure information[11] can be utilized to identify the particular *b*-hemes that are reduced in the dimeric b_6f complex.

In the present study, the time course of *b*-heme reduction in the b_6f complex, and of the increase in amplitude of the CD spectra associated with excitonic heme interactions, has for the first time been measured simultaneously. The amplitude of the absorbance spectra assays the fraction of the total *b*-heme population in the cytochrome complex that is reduced, while the split CD spectrum indicates the particular *b*-heme pair that is reduced. A difference between the midpoint redox potentials of the intramonomer hemes b_n and b_p of purified b_6f complex has been described.[19,20,53,54] Two of the studies,[19,20] utilizing a crystallizable complex from the green alga, *C. reinhardtii*,[24] that is characterized by physiological electron transfer rates of approximately 200 electrons/cytochrome *f*-s, determined a midpoint potential difference between the two hemes b_n and b_p of 75−100 mV. *In-situ* titrations of thylakoid membranes indicated that the midpoint redox potential difference could be as large as 50 mV.[55,56] Given access to and equilibration between both monomers, thermodynamics dictates that the first electrons to be transferred to the dimer would equilibrate to the higher potential *b*-heme in each of the two monomers. In the present study, however, the combined spectrophotometric and circular dichroic analysis of these electron transfer events implies that this expectation is not correct. The preferred two-electron-reduced state of the complex is the *b*-heme pair in the monomeric unit of the complex, which consists of the "high" and "low" potential hemes (b_n and b_p) defined in the redox titrations.[19,20] Consideration of the energetics implies that preferential pairwise reduction of the two *b*-hemes in the monomer would be favored only if the dielectric constant of the protein medium between the intramonomer *b*-heme pair, b_p and b_n, which have different redox potentials and which span the membrane from the electrochemically positive and negative sides, is greater than the dielectric constant $\varepsilon = 2.5$ which operates in the intermonomer space between the two higher potential (greater electron affinity) hemes b_n located in the different monomers of the complex. Thereby, the protein medium between these *b*-hemes is more polarizable than that between the two hemes b_n, whose reduction would be considered to be thermodynamically more favorable strictly on the basis of their redox potentials. Preferential reduction of the intramonomer *b*-heme pair would collect electrons into one monomer of the dimeric cytochrome b_6f complex, resulting in a more efficient reduction of the n-side bound quinone, and less efficient formation of superoxide mediated by plastosemiquinone.[57]

2. MATERIALS AND METHODS

2.1. Purification of Cytochrome b_6f Complex. The cytochrome b_6f complex was isolated from leaves of *Spinacea* as previously described.[58] The dimeric complex was separated from the monomer by size exclusion chromatography and sucrose density gradient centrifugation.[58] Densitometrry on Blue Native-PAGE to determine the relative content of monomer and dimer fractions of the b_6f complex was measured with a FluorChem E densitometer. All assays were performed in 30 mM Tris−HCl (pH 7.5), 50 mM NaCl, 0.2 mM EDTA, and 0.04% UDM (*n*-undecyl-β-D-maltopyranoside).

2.2. Electron Transfer Activity. The specific electron transfer activity of the purified cytochrome b_6f complex was measured as described previously.[59]

2.3. Measurement of Absorbance Changes; Cytochrome Difference Spectra. Absorbance spectra were measured with a Cary 4000 spectrophotometer (Varian/Agilent) in single-beam mode. For redox difference spectra, the b_6f complex was oxidized by potassium ferricyanide (50 μM). Na-ascorbate (0.25 mM) was added to reduce the relatively high potential ($E_m \approx +0.36$ V) cytochrome *f*. Reduction of the two lower potential hemes b_n and b_p associated with the cytochrome b_6 subunit of the complex was achieved by addition of an aliquot of 1 M dithionite, freshly prepared using a degassed solution of 0.1 M Tris, pH 8.0, yielding a final concentration in the cuvette of 3−4 mM ($E_{m7} \approx -0.5$ V[60]). Sufficient buffer was added to prevent a decrease in pH during the course of the measurements. A decrease in the medium pH resulted in a significantly increased rate of *b*-heme reduction (>10-fold at pH < 6.0). The state associated with complete heme reduction is stable for 30 min, indicating maintenance of anaerobic conditions. Concentrations of cytochromes *f* and b_6 were calculated from the amplitude of the redox difference absorbance spectrum (ascorbate-reduced minus ferricyanide-oxidized) at 554 or 563 nm (dithionite-reduced minus ascorbate-reduced), respectively, using extinction coefficients of 25 and 23−25 mM^{-1} cm^{-1} determined for difference spectra of cytochromes *f*[61] and b_6.

2.4. Low Temperature (77 K) Determination of *b*-Heme Spectra. Upon addition of dithionite to b_6f complex suspended in a detergent solution containing 50% glycerol, small aliquots (0.8 mL) were frozen in liquid nitrogen. The absorbance was monitored using a UV−vis Cary 300 Bio (Varian) spectrometer with a measuring beam half-bandwidth of 0.2 nm.

2.5. Simultaneous Measurement of Circular Dichroism and Absorbance Spectra. Soret band CD spectra and

dx.doi.org/10.1021/jp501165k | J. Phys. Chem. B 2014, 118, 6614−6625

absorbance spectra of the b_6f complex were measured simultaneously in a cuvette with 1 cm optical path length and magnetic stirring, with a half-bandwidth of 1 nm, using a "Chirascan" (Applied Photophysics, Ltd., U.K.) spectropolarimeter equipped with thermal control and magnetic stirring of samples. Dithionite as reductant was added as described above in section 2.3, and consecutive spectra were collected at intervals of approximately 16 s.

2.6. Structure-Based Calculation of Circular Dichroism Spectra Derived from the Set of Heme−Heme Excitonic Interactions. Simulations of CD spectra for all four possible pairs of reduced *b*-hemes of the dimeric cytochrome b_6f complex were performed using a formalism previously described.[51] The dipole−dipole coupling potential, V_{12} (in cm^{-1}), between the optical transitions of two spectroscopically identical chromophores can be expressed as eq 1:

$$V_{12} = \frac{5040}{R_{12}^{3}}[\vec{\mu}_1\cdot\vec{\mu}_2 - 3(\vec{\mu}_1\cdot\hat{r})(\vec{\mu}_2\cdot\hat{r})] \quad (1)$$

where R_{12} is the center−center distance (in Å) between the two hemes, $\hat{r}$ is a unit vector in the direction of R_{12}, and $\vec{\mu}_1$ and $\vec{\mu}_2$ are the transition dipole moments of the two interacting hemes expressed in Debye units, 3.34×10^{-30} C-m. The numerical coefficient 5040 in eq 1 results from the use of Debye units and expression of the coupling potential, V, in cm^{-1}.[51] The interaction between the two hemes causes a separation of the absorbance band into two excitonically split bands with maxima at energies ν_+ and ν_-, as described by eq 2:

$$\nu_{\pm} = \nu_0 \pm V_{12} \quad (2)$$

where ν_0 is the transition energy of a noninteracting heme. Following the notation of Palmer et al.,[51] the rotational strength, in Debye units, of the two transitions is described by eq 3:

$$R_{\pm} = \frac{170}{\lambda}R_{12}[\hat{r}\cdot(\hat{\mu}_1 \times \hat{\mu}_2)] \quad (3)$$

where λ is the optical transition wavelength, in Å. The optical CD signal as a function of wavelength was calculated by adding two Gaussian bands that mimic the shape of the *b*-heme absorbance. One of amplitude R_+ is centered at ν_+, and the other of amplitude R_- is centered at ν_-. Equations 1−3 have been used to derive expressions for CD signal strength expressed in terms of the interplanar angles between the *b*-hemes.[51] The angular information required for eqs 1−3 for calculation of the interaction energy and the CD signal was derived from the crystal structure of the b_6f complex (PDB ID 4H44). The Q_x and Q_y transitions of the reduced *b*-hemes are known to point along the directions between nitrogens, N_A−N_C and N_B−N_D (Table S1, Supporting Information), respectively, and the distances between the pairs of *b*-hemes were calculated as Fe−Fe distances derived from the crystallographic structure (PDB ID 4H44) (Figure 1B; Table 1). The transition moment of each transition was set to be 4.6 D.[51] Since the heme Q_x and Q_y transitions are degenerate, the CD spectra of all four interacting transitions between two *b*-hemes (Q_x−Q_x, Q_x−Q_y, Q_y−Q_x, Q_y−Q_y) were calculated separately and then combined. As the goal of these simulations was estimation of the relative contribution of each *b*-heme pair to the CD spectrum, the absorbance spectrum of each *b*-heme was modeled as a Gaussian band with a half-width of approximately 10 nm.

3. RESULTS

Purified predominantly dimeric cytochrome b_6f complex, prepared as described, was obtained by hydrophobic chromatography and separated from inactive monomer by size exclusion chromatography (Materials and Methods). The dimeric character of the isolated complex was confirmed by clear native gel electrophoresis analysis, its subunit composition defined by SDS-PAGE analysis (Figure S2A, Supporting Information), and its electron transfer rate from donor decylplastoquinol to the plastocyanin/ferricyanide determined (150−200 electrons-cyt f^{-1}-s^{-1}). Monomeric b_6f complex prepared as described in the Materials and Methods section, and displayed by native gel electrophoresis in Figure S2B of the Supporting Information, was inactive.

3.1. Dithionite Reduction of Hemes b_n and b_p; Room Temperature and 77 K. The *b*-hemes in the dimeric b_6f complex are completely reduced in a pH-dependent reaction by dithionite (3−4 mM) in 10−12 min (room temperature, 23 °C) at pH 7.5 (Figure 2A and B). The rate of heme *b* reduction by dithionite at pH 8.0 was approximately 100-fold slower compared with that at pH 5. The fully reduced state was stable for at least 30 min. Absorbance spectra measured at 77 K resolve the presence of hemes *f*, b_n, and b_p (Figure S3, Supporting Information), with the dithionite-minus-ascorbate difference spectrum defining the spectra of hemes b_n and b_p. Dithionite addition was performed under anaerobic conditions. On the basis of the area under the domains of the low temperature (77 K) difference spectra in the α-band region that arise from hemes b_6 and *f* (Figure S3, Supporting Information), the measured molar ratio of heme *b* to heme *f* was 2.0:1.

3.2. Simultaneous Measurement of Circular Dichroism (CD) and Absorbance Spectra. Soret band CD spectroscopy, utilized as described elsewhere[51] and in section 2.6 in the Materials and Methods section, has been previously used to describe exciton interactions between *b*-hemes of respiratory cytochrome bc_1,[51,62,63] and in studies on the *C. reinhardtii* photosynthetic b_6f complex,[52] although the identity of the interacting hemes was not determined. The basis for the method rests on the net transition dipole moment of two or more individual transition moments in a molecular array resulting from superposition of the individual moments. The net polarization of circularly polarized light results from preferential absorption of right- and left-hand polarized light by the array.[64]

The time course of *b*-heme reduction measured by the Soret band absorbance change at room temperature (Figure 2A and B) and of heme−heme exciton interaction, assayed by CD spectra (Figure 2C) of active dimer, are experimentally indistinguishable (Figure 2D). As in the previous CD studies on the bc_1[51] and b_6f[52] complexes, the amplitude of the short wavelength (428 nm) positive lobe of the split CD spectrum is approximately 20% larger than the longer wavelength negative lobe centered at 436 nm[52] (Figure 2C). In the b_6f complex, this asymmetry could be a consequence of a CD signal arising from the reduction of the unique heme c_n, identified in refs 12, 24, and 29, whose Soret band maximum in the reduced state is approximately 424 nm.[19] However, neither heme c_n nor any features unique to b_6f compared to bc_1 are likely to be the source of this asymmetry, as the asymmetry is similar in the CD spectra of the bc_1 complex[51] in which heme c_n is absent. The normalized CD spectra of monomer and dimer are similar (Figures 3, Figure S4, Supporting Information), implying that

dx.doi.org/10.1021/jp501165k | J. Phys. Chem. B 2014, 118, 6614−6625

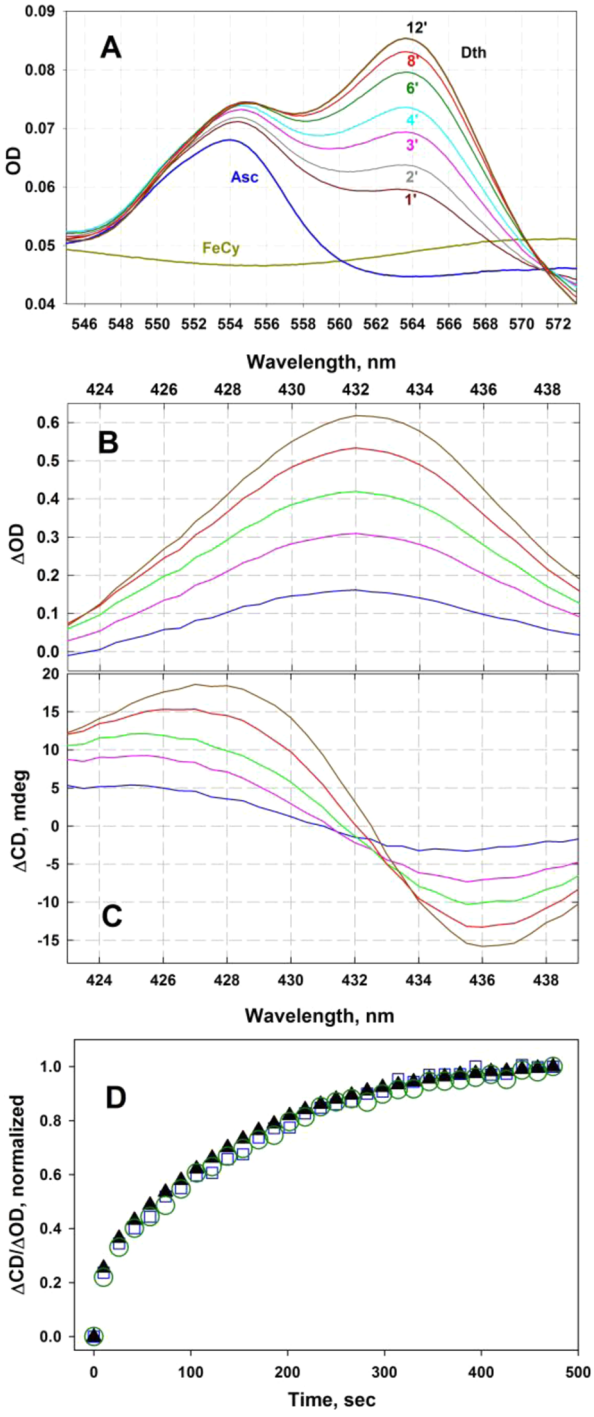

Figure 2. Absorbance spectra of dithionite-reduced cytochrome b_6f complex; simultaneous kinetics of reduction of hemes b_n and b_p in dimeric b_6f complex. (A) Room temperature α-band absorbance spectra of cytochromes f and b_6, with room temperature absorbance spectra, respectively, at 554 and 563 nm, as a function of time of dimeric b_6f complex initially oxidized by ferricyanide (FeCy; 20 μM), reduced by ascorbate (Asc; 0.1 mM), and reduced subsequently by dithionite (Dth, final concentration 2−3 mM). Buffer, 30 mM HEPES, pH 7.5, 50 mM NaCl, 0.1 mM EDTA, 0.045% UDM. Dimeric b_6f complex containing 0.8 μM cytochrome f. (B, C) Time course of (B) heme b reduction by dithionite and (C) increase in amplitude of the split CD spectrum in dimeric b_6f complex; kinetics of heme b reduction by dithionite. The dimeric b_6f complex contained 1.6 μM cytochrome f. Dithionite was added to a concentration of 3−4 mM, and 27 consecutive OD and CD spectra (420−440 nm) were simultaneously measured (16 s per spectrum). Measurement of all CD and OD difference spectra was started 10 (blue), 74 (pink), 138 (green), 234 (red), and 410 (brown) s after addition of dithionite. (D) Measured kinetics induced by dithionite addition to the dimeric b_6f complex: absorbance increase at 432 nm (triangles, black); amplitude of Soret band circular dichroism (CD) signals at 428 nm (circles, blue) and 437 nm (squares, blue).

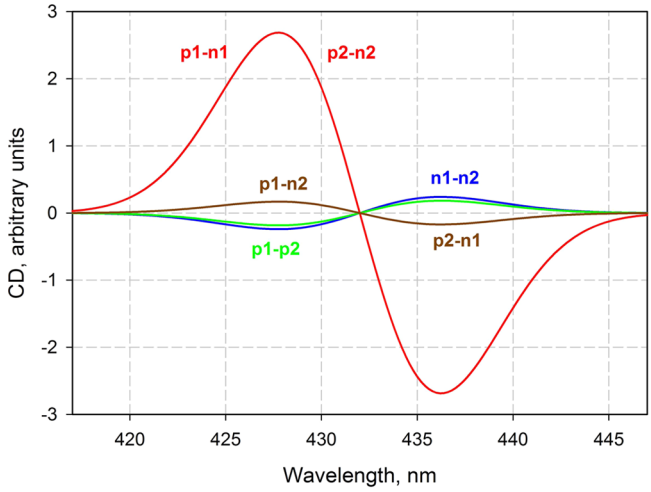

Figure 3. Calculated CD interaction between all reduced heme pairs: p1−n1 or p2−n2 (red trace), which are the dominant interactions; calculated spectra are shown for the other heme pairs, p1−n2, p2−n1 (purple), p1−p2 (blue), and n1−n2 (green).

the major excitonic interaction responsible for the split CD spectrum arises from the two intramonomer hemes, b_p and b_n. This conclusion is in excellent agreement with the CD spectra calculated from the information available from crystal structures on interheme distances and dihedral angles (Materials and Methods, section 2.6), shown in Figure 3. The major source of the split CD signal (Figure 2C, Figure S4, Supporting Information) is the interaction between the intramonomer b-heme pairs on the electrochemically positive (p) and negative (n) sides of the membrane, p1−n1 and p2−n2 (red trace). Significantly smaller CD signals are expected from all other b-heme pairs (Figure 3, Table 1). Table 1 summarizes the relative intensities of CD signals from all six interacting pairs formed by the four b-hemes.

3.3. Preferential Reduction of the Intramonomer b_n−b_p Pair; Mechanism of Dithionite Reduction. Using a common measuring beam in the combined spectrophotometer/polarimeter described in Materials and Methods, simultaneous measurement was made of the kinetics of the absorbance changes (Figure 2D) at 432 nm (red, triangles) associated with b-heme reduction, and of the ellipticity changes of the Soret band split CD signal, measured at 428 nm (circles) and 437 nm (blue, squares), associated with heme−heme excitonic interactions. The similarity of these kinetics indicates that the two processes are occurring coincidentally on the time scale of the measurement. The slow time course of dithionite reduction of the b-hemes is attributed to the electrostatic barrier presented to anionic dithionite by the low dielectric medium of the protein interior of the complex, which can also be observed as a Stark effect sensed by the chlorophyll-a molecule present in each monomer.[65] It is noted that dithionite is much

dx.doi.org/10.1021/jp501165k | J. Phys. Chem. B 2014, 118, 6614−6625

less permeable in the hydrophobic cytochrome complex than is the physiological protonated plastoquinol or semiquinone reductant, which are also substantially weaker reductants.

The ratio of the slow and fast kinetic components characterizing the kinetics of the absorbance and CD changes (Figure 2D) is similar to the ratio of monomer to dimer complex in the fractions separated by size exclusion chromatography and analyzed by SDS-PAGE and native gel electrophoresis (Figures S2A and B, Supporting Information). The absorbance data is described by a double exponential, having rate constants for fast and slow components of 0.18 ± 0.02 s^{-1} (22%) and 0.006 ± 0.001 s^{-1} (78%). In addition, to explain the coincident time course of the CD and absorbance changes, an explanation is needed of the mechanism by which four electrons are transferred to the complex.

3.4. Model of the Observed CD and Absorbance Dynamics. The rate of electron transfer to the cytochrome complex, k, is assumed to be limited by the diffusion rate of the donor molecule (dithionite) to the complex and thus is independent of the redox state of the complex. Assuming that dithionite is a one-electron donor, four electron transfer steps are required to completely reduce the initially oxidized four b-heme complex, as described by eq 4 below:

$$\boxed{N_0(t)} \xrightarrow[\bar{e}]{k} \boxed{N_1(t)} \xrightarrow[\bar{e}]{k} \boxed{N_2(t)} \xrightarrow[\bar{e}]{k} \boxed{N_3(t)} \xrightarrow[\bar{e}]{k} \boxed{N_4(t)} \quad (4)$$

$N_i(t)$ represents the time-dependent population state of the dimeric complex with subscript i denoting the number of reduced b-hemes. The system of kinetic equations can be solved analytically, as shown for the case of one-electron transfer (eq S3, Supporting Information). Since the time scale of reduction of the complex by the donor (~100 s) is much slower than intracomplex electron transfer between the b-hemes (~1 ms), it is assumed that the electrons in the complex adopt the thermodynamically most probable configuration, i.e., that with the lowest free energy. The absorbance (OD) signal, $\mathrm{OD}(t)$, reflects the total population of the reduced b-hemes, i.e., $\mathrm{OD}(t) \sim [N_1(t) + 2N_2(t) + 3N_3(t) + 4N_4(t)]$, and does not depend on the order in which the b-hemes are reduced. The CD signal kinetics, $\mathrm{CD}(t)$, however, depend on the order in which the b-hemes are reduced, because reduction of the intramonomer b_n and b_p hemes is uniquely required for a CD signal of significant amplitude (Table 1, Figure 3). If these two intramonomer b-hemes are the first to be reduced, the CD signal will increase faster than if any other heme pair is populated first (Figure 4). Thus, two models are considered:

(i) "n−n" model (Figure 5A): the lowest doubly reduced state of the dimer corresponds to two electrons residing on the two b_n hemes on the electrochemically negative side of the membrane that belong to different subunits. In that case, three electron transfer steps are needed to observe a significant increase in the CD signal that would arise from a reduced n−p pair.

(ii) "n−p" model (Figure 5B): the lowest doubly reduced state of the dimer corresponds to two electrons residing on the b_n and b_p hemes belonging to the same monomer. In this case, two electron transfer events will result in a significant increase of the CD signal.

The CD signal kinetics for different models are calculated according to the population of different pairs of b-hemes and their CD yields (Table 1, eq S5 and Figure S5, Supporting Information). The measured absorbance difference was fit using kinetic scheme 4, assuming the presence of two different pools of b_6f complexes with different rate constants, k. The best fit is shown in Figure 4. In addition, the CD signals expected for the two models are plotted and compared against the measured CD kinetics. The faster rate, which is comparable with the time resolution of the experiment, is attributed to "contaminant" monomer complex in the dimer preparation (Figure S2A, Supporting Information, native gel), and the slower rate is assigned to the reduction dynamics of the dimeric complex. The "n−n" model predicts that the CD signal from the dimer should be significantly delayed (~100 s, Figure 4, red curve), which contradicts the experimental measurement. A reasonable agreement with experiment is observed only for the "n−p" model (Figure 4, blue curve).

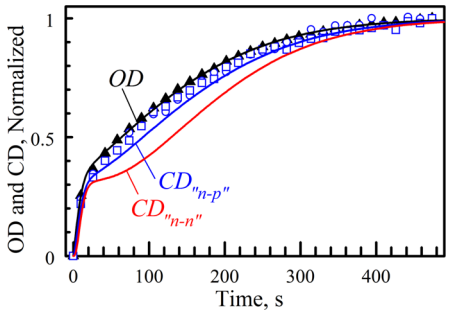

Figure 4. CD (circles, squares, blue) and optical density changes (triangles, black) were measured simultaneously, as described in the Materials and Methods section. Solid curves are kinetic simulations as described in the Results section, with the assumption that dithionite acts as a one-electron donor; the predicted time course for dithionite acting as a two-electron donor is shown in Figure S7 (Supporting Information). Electron transfer to the b_6f dimer is described by two rate constants: k_1 = 0.017 s^{-1} (70%) and k_2 = 0.33 s^{-1} (30%); the larger rate constant is attributed to "contaminant" monomer complex in the dimer preparation (Figure S2B, Supporting Information, native gel). Black curve: fit to measured absorbance changes (triangles). Blue curve: expected CD kinetics in the "n−p" model where the intermediate doubly reduced intramonomer (Figure 5B; state N_2) dimer has a lower free energy than the intermonomer doubly reduced state in which heme b_n is reduced in both monomers (Figure 5A; state N_2). Red function: expected time course of the CD change in the "n−n" model in which the intramonomer n1−n2 doubly reduced state has the lowest free energy.

Dithionite can also act as a two-electron donor[66] (Figure 5A and B), in which case the following kinetic scheme (eq 5) describes the OD and CD signals:

$$\boxed{N_0(t)} \xrightarrow[2\bar{e}]{k} \boxed{N_2(t)} \xrightarrow[2\bar{e}]{k} \boxed{N_4(t)} \quad (5)$$

The analytical solution for the respective system of kinetic differential equations is provided in the Supporting Information (eq S7), and the respective fit of OD and CD signals for the "n−p" and "n−n" models is shown (Figure S6, Supporting Information). The predicted delay in the time course of the CD signal in the "n−n" model is almost identical for the case of a one- and two-electron donor (compare Figure 4 and Figure S6, Supporting Information), and disagrees with the experimental data. It is important to note that, if dithionite acts as a mixture of one- and two-electron donors,[66] a close fit of the time course of OD and CD signals can be achieved within the "n−p" model, while the "n−n" model contradicts the data (Figure S7, Supporting Information).

Thus, independently of whether dithionite donates one or two electrons, the "b_n−b_p" model ("n−p" in Figure 5) uniquely predicts the relative time course of the absorbance and CD

dx.doi.org/10.1021/jp501165k | J. Phys. Chem. B 2014, 118, 6614−6625

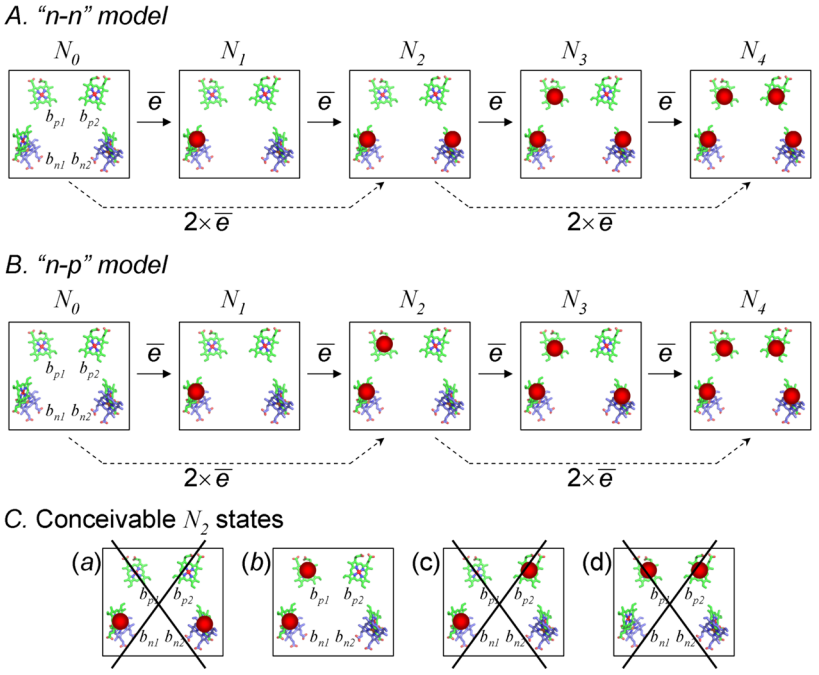

Figure 5. Summary of possible electron transfer routes and heme reduction states in the b_6f complex. Two different models are considered: (A) n1−n2 model: the doubly reduced state of lowest energy of the dimer corresponds to two electrons residing on the two b_n hemes belonging to different subunits (this state produces a weak negative CD signal (Figure 3). (B) n−p model: the lowest doubly reduced state of the dimer corresponds to two electrons residing on the b_n and b_p hemes belonging to the same subunit (in this state, the amplitude of the positive CD signal is significantly larger than that of any other heme pair). The sequence of four electron transfer events in these two models is illustrated. Reduced hemes are shown as red spheres. State N_0 in panels A and B denotes fully oxidized hemes in dimeric complex. N_i represent states of the dimeric complex in which subscript "i" represents the number of reduced hemes. States N_1 and N_3 are bypassed if dithionite acts as a 2 e^- donor. (C) Summary of conceivable two electron half-reduced states, of which the three states marked by "X" are inferred to be substantially less probable, although they have been documented to exist (refs 14, 15, 17, 19, 21, and 26).

signals. Thus, in the most stable two electron-reduced state of the dimeric cytochrome b_6f complex, the two electrons preferentially reside in the intramonomer b-heme pair, b_n−b_p. The half-reduced mixed intermonomer states summarized in Figure 5C, panels a, c, and d (states marked "X"), are relatively improbable at thermal equilibrium, although certainly realizable in studies on the time course and mutational alteration of electron transport in the cytochrome bc_1 complex.[36,39−41,43,47]

4. DISCUSSION

4.1. The Preferential "b_n−b_p" (n−p) Model; Thermodynamic Considerations Modified by Electrostatic Interactions. The contradiction to the expectation, based on elementary thermodynamics, that the two higher potential b-hemes (b_n) provide the most stable two-electron-reduced state of the heme pairs in the dimeric cytochrome complex lies in the electrostatic interactions that result from injection of electronic charge into a low dielectric medium. The preferred residence of electron pairs on one monomer is not a consequence of electron transfer to the other monomer in the dimer being blocked in any conceivable way but results from the reduced intramonomer b-heme configuration being the lowest energy state for the two-electron-reduced dimer.

4.2. Consequences for Heterogeneity of Dielectric Constant in the Cytochrome b_6f Complex. The preferential reduction by dithionite of the intramonomer hemes b_n and b_p can be explained only if the dielectric constants are not equivalent between the different b-heme pairs summarized in Figure 5, and if the local dielectric constant between the intramonomer hemes b_n and b_p is relatively high (Figure 6). Thus, the structure of the photosynthetic b_6f complex is characterized by internal dielectric heterogeneity. The nature of the dielectric phenomena in the interior of proteins has been discussed.[67] Dielectric heterogeneity in hetero-oligomeric membrane protein complexes involved in photosynthetic energy transduction has been inferred previously in the hetero-oligomeric bacterial[33,68−70] and photosystem I reaction centers.[33,71]

4.3. Boundary Conditions for Dielectric Heterogeneity. The data indicate that the two electrons transferred to a monomer (Figure 5B; N_2 panel) do not spill over to the neighboring monomer (Figure 5C) within the several minute time span of the measurements. Because intermonomer electron transfer between the two b_p-hemes in the dimer is expected to be on the order of microseconds (edge-to-edge distance, 12.8 Å), there is sufficient time for energetic equilibration between all possible forms of a doubly reduced dimer (Figure 5C), unless there is an energetic mechanism that precludes electron transfer between the monomers. Since the latter is improbable, it is inferred that the intramonomer reduced heme b_p−b_n pair (Figure 5B, N_2 panel; Figure 5C, state b) corresponds to the lowest energy configuration. The total energy E_{ij} of this pair can be expressed as eq 6:

$$E_{ij} = E_i + E_j + V_{ij} \tag{6}$$

where E_i and E_j are the energies of noninteracting electrons in sites i and j, respectively, and are defined by the redox potentials of the respective b-hemes. V_{ij} is the Coulombic interaction energy between these two electrons, which, as shown below, can be comparable or larger than the difference

dx.doi.org/10.1021/jp501165k | J. Phys. Chem. B 2014, 118, 6614−6625

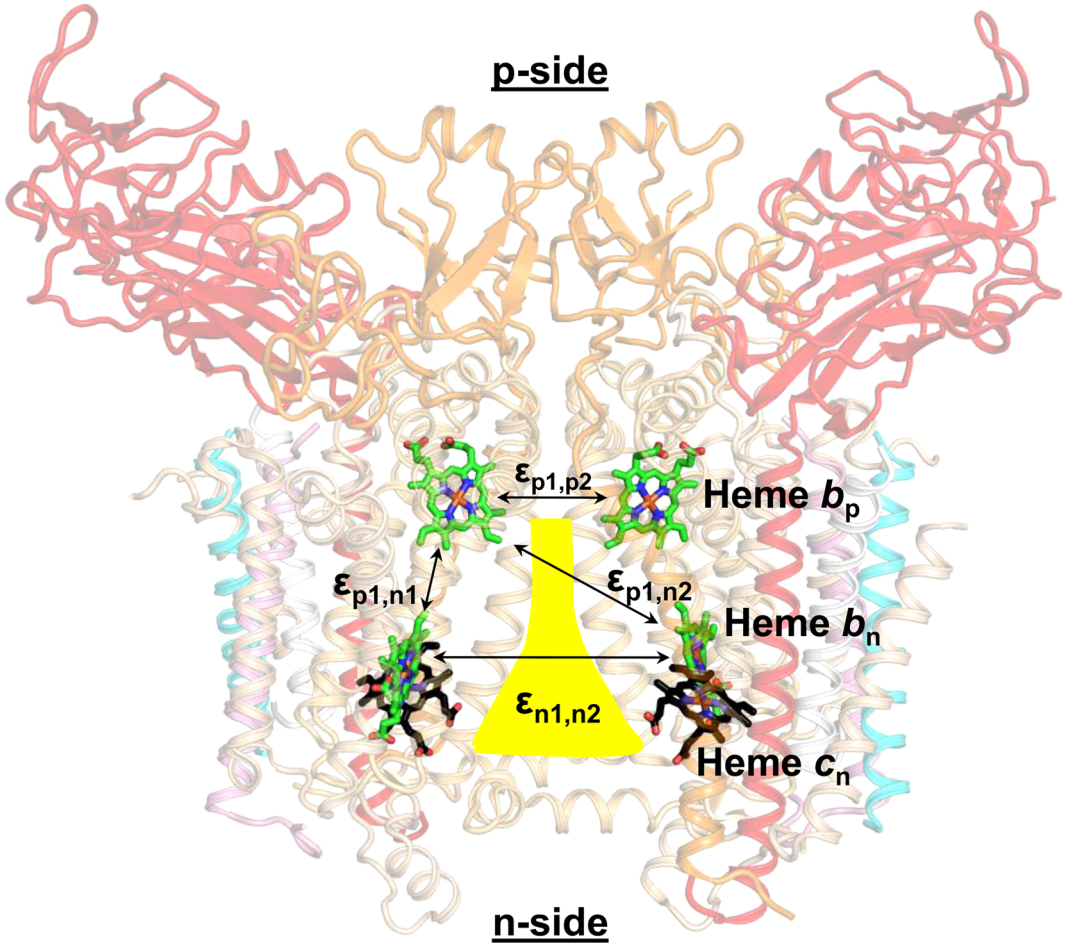

Figure 6. Description of dielectric heterogeneity in the cytochrome b_6f complex (PDB ID 4H44). Four interheme dielectric constants, which have different values, are shown: (i) the reference dielectric constant, $\varepsilon_{n1,n2} \equiv 2.5$[15] between the two n-side hemes that bridge the major intermonomer cavity (yellow) that contains a high concentration of lipid (Hasan et al., submitted for publication), (ii) $\varepsilon_{n1,p1} = \varepsilon_{n2,p2}$ between the intramonomer hemes, (iii) $\varepsilon_{p1,n2} = \varepsilon_{p2,n1}$ between the p-side heme on one monomer and the n-side heme on the other, and (iv) $\varepsilon_{p1,p2}$ between the two p-side hemes. The minimum values of ε necessary for the energetically favored reduction of a particular heme pair among the four possible pairs in the dimeric complex, dependent upon the midpoint redox potential difference (ΔE_m) between hemes b_n and b_p (50, 75, and 100 mV), calculated to the nearest half-integral values using the reference dielectric constant for $\varepsilon_{n1,n2}$ of 2.5 and eq 9 are, respectively, $\varepsilon_{n1,p1} = \varepsilon_{n2,p2} > 6.1$, 7.8, and 10.8 (Table 2). The corresponding values for the electrostatic interaction between the two hemes on different monomers on opposite sides of the complex, $\varepsilon_{n1,p2} = \varepsilon_{n2,p1}$, are >3.7, 4.7, and 6.6. Energetically preferred reduction of the p-side heme pair, p1 and p2, corresponding to a ΔE_m between hemes b_n and b_p of 50 and 75 mV, respectively, would require dielectric constants >10.1 and >43.6.

in redox energy between the two hemes in the complex. If the dielectric constant is $\varepsilon = 2$, then the electrostatic interaction energy between two hemes in the complex is on the order of 0.2−0.3 eV.

The indices i and j correspond to the reduction of one of the four b-hemes: i, j = n1, p1, n2, p2, where n1, p1 denote hemes b_n and b_p in one monomer and n2, p2, the pair in the second monomer of the dimeric complex. The electrostatic interaction energy in a point-charge approximation, described by Coulomb's law, is obtained from eq 7 below:

$$V_{ij} = \frac{1}{4\pi\varepsilon_0\varepsilon_{ij}}\frac{e^2}{R_{ij}}, \quad i \neq j \tag{7}$$

where e is the charge of an electron, R_{ij} is the distance between two electrons, ε_0 is the permittivity of free space, and ε_{ij} are the effective dielectric constants that operate between any heme pair, b_i and b_j. The above eq 7 can then be rewritten as eq 8:

$$V_{ij}\ [\mathrm{eV}] = \frac{14.4\ [\text{Å}\cdot\mathrm{eV}]}{\varepsilon_{ij}R_{ij}}, \quad i \neq j \tag{8}$$

with the units of R_{ij} in Å, the resulting V_{ij} expressed in electron-volts (eV), and the dimensions of the numerator, Å·eV. The R_{ij} are the center-to-center distances between the respective hemes: $R_{n1,p1}$ = 21 Å, $R_{n1,p2}$ = 34 Å, $R_{n1,n2}$ = 35 Å, and $R_{p1,p2}$ = 22 Å (Table 1); ε_{ij} is the corresponding dielectric constant between these heme pairs. The consensus values of midpoint redox potentials, E_m, of hemes b_p and b_n in isolated active (≥200 electrons transferred/cytochrome f-s) cytochrome b_6f complex, measured in vitro and in situ, differ by 0.05−0.1 V, with heme b_p having the more negative potential.[19,20,55,56,72] In intact thylakoid membranes, ΔE_m has been found to be approximately 0.1 V[72] or as large as 0.05 V.[55,73] Thus, defining the energy of the reduced heme b_n as $E_{n1} = E_{n2} = 0$, the energy of the reduced heme b_p will be $E_{p1} = E_{p2}$ = 0.05−0.1 eV corresponding to the difference, ΔE_m, in midpoint potential of hemes b_n and b_p. Using formulas **6** and **8**, and taking ΔE_m into account, the energies (in electron-volts, eV) for all possible

dx.doi.org/10.1021/jp501165k | J. Phys. Chem. B 2014, 118, 6614−6625

doubly reduced states of the dimeric complex shown in Figure 5C are obtained from eq 9.

$$\begin{cases} E_{n1,n2} = \dfrac{14.4\ [\text{Å}\cdot\text{eV}]}{\varepsilon_{n1,n2} R_{n1,n2}} & \text{(state a)} \\ E_{n1,p1} = E_{n2,p2} = \Delta E_m\ [\text{eV}] + \dfrac{14.4\ [\text{Å}\cdot\text{eV}]}{\varepsilon_{n1,p1} R_{n1,p1}} & \text{(state b)} \\ E_{n1,p2} = E_{n2,p1} = \Delta E_m\ [\text{eV}] + \dfrac{14.4\ [\text{Å}\cdot\text{eV}]}{\varepsilon_{n1,p2} R_{n1,p2}} & \text{(state c)} \\ E_{p1,p2} = 2\Delta E_m\ [\text{eV}] + \dfrac{14.4\ [\text{Å}\cdot\text{eV}]}{\varepsilon_{p1,p2} R_{p1,p2}} & \text{(state d)} \end{cases} \quad (9)$$

The equations for states (b−d) contain two terms: the first term describes the difference in midpoint redox potential, ΔE_m, in units of eV (states b, c), between the n- and p-side *b*-hemes, and $2\Delta E_m$ (state d), the total difference in midpoint potential between the two p-side and n-side *b*-hemes in the complex. The second term on the right-hand side of the formulas for states b−d, and the term on the right sides of the formula for state a, describes the Coulombic interaction between the *b*-hemes in a point charge approximation.

The constraint on the dielectric constants that result in a Coulombic interaction energy $E_{n1,p1}$ or $E_{n2,p2}$ level between the two trans-membrane hemes b_n and b_p in each monomer being lower than that between the two high potential hemes, $E_{n1,p1}$, is

$$\varepsilon_{n1,p1} = \varepsilon_{n2,p2} > \varepsilon_{n1,n2} \quad (10)$$

where $\varepsilon_{n1,n2}$ is the dielectric constant between the two hemes b_n. $\varepsilon_{n1,n2}$ is assumed to be close to the minimum value inferred to exist in a protein, ε = 2.5,[15] because (i) the protein is embedded in a membrane, and (ii) the intermonomer cavity between the hemes b_n contains a significant lipid content, as depicted in Figure 6. Values of $E_{n1,p1} = E_{n2,p2}$ that satisfy this inequality for ΔE_m values of 0.05, 0.075, and 0.1 V are >6.1, 7.8, and 10.8 (Table 2). For the same set of ΔE_m values, the local dielectric constants that would render most probable (a) the intermonomer, interheme pathways, are $\varepsilon_{n1,p2} = \varepsilon_{n2,p1} > 3.7$, 4.7, and 6.6; for ΔE_m values of 0.05 and 0.075 V, $\varepsilon_{p1,p2} > 10.1$ and 44. It is important to note that the energetic preference for reduction of the intramonomer heme pairs (b_{n1}, b_{p1} and b_{n2}, b_{p2}) implies that the values of the dielectric constants, ε, between the other heme pairs, b_{n1}, b_{p2}, b_{n2}, b_{p1}, and b_{p1}, b_{p2} are smaller than the values presented in Table 2.

Table 2. Threshold Interheme Dielectric Constants (ε) in the Dimeric Cytochrome b_6f Complex[a]

	$\varepsilon_{n1,n2}$ = 2.5		
ΔE_m (mV)	$\varepsilon_{n1,p1}$	$\varepsilon_{n1,p2}$	$\varepsilon_{p1,p2}$
50	≥6.1	≥3.7	≥10.1
75	≥7.8	≥4.7	≥43.6
100	≥10.8	≥6.6	*

[a]As shown in Figure 6: $\varepsilon_{n1,n2}$, dielectric constant between hemes b_{n1} and b_{n2}, $\varepsilon_{n1,p1}$ (=$\varepsilon_{n2,p2}$), dielectric constant between hemes b_{n1} (or b_{n2}) and b_{p1} (or b_{p2}); $\varepsilon_{n1,p2}$ (=$\varepsilon_{n2,p1}$), dielectric constant between hemes b_{n1} (or b_{n2}) and b_{p2} (or b_{p1}); $\varepsilon_{p1,p2}$, dielectric constant between hemes b_{p1} and b_{p2}; ΔE_m, mid-point redox potential difference between hemes b_p and b_n; *, given an unfavorable redox potential difference for storage of two electrons on the two hemes b_p, there is no value of the dielectric constant that will satisfy this state.

4.4. The Preferential Intramonomer Electron Transfer Pathway; Interheme Distance Considerations. If the elevated dielectric constant (>6.1) between the intramonomer hemes b_n and b_p provides the explanation for the preferential heme reduction of the intramonomer heme pair, the question arises as to why reduction of the intermonomer heme pair, b_{p1}−b_{n2} or b_{p2}−b_{n1}, is disfavored if the constraint on this interheme dielectric constant, ε > 4, is less stringent. The low probability of utilization of the latter electron transfer pathway is a consequence of the steep donor−acceptor distance dependence of intraprotein electron transfer[31−35] and the much greater distance, 22.3 Å, between the intermonomer heme rings compared to 8.1 Å between the intramonomer pair (Figure 1B). Although the interheme distance, 12.8 Å (Figure 1B), does not preclude interheme electron transfer, preferred reduction of the heme b_{p1}−b_{p2} pair is rendered extremely unlikely because of the requirement of a dielectric constant of ≥44, substantially approaching that of bulk water. This extreme constraint is a consequence of the large free energy surplus in the two hemes b_p, resulting from the appreciable (75 mV in this calculation) redox potential difference between hemes b_p and b_n. See the note in Table 2 regarding the case of ΔE_m = 100 mV. It should be noted that the above dielectric constants are not absolute but are referenced to an assumed dielectric constant of 2.5 in the lipid-containing intermonomer space between the two hemes b_n, whose rationale is discussed above.

4.5. Origin of Heterogeneous Dielectric Constants: Reorganization Energy Associated with Electron Transfer; Heterogeneity in the Structure. The existence of heterogeneous dielectric constants in electron transferring membrane proteins is not unprecedented. The local dielectric constants in the electron transfer pathways of the multisubunit hetero-oligomeric photosynthetic reaction centers can be higher[74] than the values ($\varepsilon \approx 2.5$−4) assigned to a dry folded protein.[15] A value of ∼7 was found for the region of the protein surrounding the electron transfer chain in PS I,[71] and local values of 4.5−4.7[70] and 10[69] inferred along the active electron transfer branch of the bacterial photosynthetic reaction center complex. The heterogeneity can be a consequence of structure reorganization associated with electron transfer, described locally in an electron transfer pair by a reorganization energy.[75,76]

The structural origin of the heterogeneity of the dielectric constant of the cytochrome b_6f complex can be attributed to several features of the protein complex: (a) The arrangement of the α-helices in the structure is intrinsically anisotropic, as is true of all helical membrane proteins; (b) a heterogeneous environment could arise from the nonuniformity introduced by lipids intercalated between subunits in these proteins, as documented for the b_6f[77] and bc_1[7] complexes. In the case of the dimeric b_6f complex, the intramonomer hemes b_p and b_n are embedded within a protein environment, while the two b_n-hemes are separated by a large, apolar intermonomer cavity (Figure 6), which is expected to lower the effective dielectric constant between the b_n-hemes. Thus, it is expected that the reduction of the intramonomer heme b_p−b_n pair would be energetically more favorable than the reduction of the intermonomer heme b_n−b_n pair.

dx.doi.org/10.1021/jp501165k | J. Phys. Chem. B 2014, 118, 6614−6625

4.6. Consequences of Dielectric Heterogeneity for Efficiency of the Trans-Membrane Electron Transfer Pathway. It has been found that electrons can cross over from one monomer to the other in the dimeric cytochrome bc_1 complex.[40,41,43,47] In the present study, it is inferred that the most probable pathway for transfer of the two electrons donated by plastoquinol on the p-side of the complex to the n-side, where they are utilized for quinone reduction, is via a transfer that is effectively pairwise through the heme pair, b_p and b_n. The existence of a preferred intramonomer pathway does not contradict the experimental documentation that electrons can cross over between the two monomers of the dimeric complex[40,41,43,47] at the level of heme b_p. Electrons injected into different monomers in the dimeric complex on the p-side are expected to merge to one of the monomers, the most stable doubly reduced thermodynamic state.

4.7. Further Consequences for Function. It is concluded that, if two electrons are injected into different monomers of the dimeric complex, the electrons tend to cross over into one monomer, which represents the most stable thermodynamic state. Thus, electron transfer across the trans-membrane domain of the b_6f complex is expected to proceed through the monomer to the quinone bound on the n-side, whose reduction would then require only two p-side quinol oxidation events. Alternatively, if reduction of the two b_n-hemes represented the most stable thermodynamic state of a two-electron-reduced b_6f dimer, then up to three p-side quinol oxidation events could be required to provide two electrons for n-side quinone reduction. The p-side quinol deprotonation−oxidation reactions are known to contain the slow, millisecond rate-limiting charge transfer step in cytochrome *bc* complexes.[78,79] Due to the more stable environment for an electron pair within the b_6f monomer, the requirement for slow p-side quinol reactions is decreased from three to two, thereby increasing the efficiency of the complex. As described elsewhere, electron transfer within the cytochrome complex may thus be essential to reducing the lifetime of unpaired electrons, which can leak to oxygen to form possibly deleterious superoxide.[57]

■ ASSOCIATED CONTENT

Supporting Information

Documentation is presented underlying a new perspective, a mapping of internal dielectric constants, for analyzing the internal structure of hetero-oligomeric integral membrane proteins. In a framework describing the b-heme centers in the core of the cytochrome b_6f complex, and electrophoretic and spectrophotometric characterization of the complex, simulations are presented of the time course of formation of absorbance and CD changes arising from dithionite reduction of the hemes, which document that the intramonomer heme pair is preferentially reduced. This material is available free of charge via the Internet at http://pubs.acs.org.

■ AUTHOR INFORMATION

Corresponding Authors

*Phone: 765-494-0706. E-mail: sergei@purdue.edu.
*Phone: 765-494-4956. E-mail: waclab@purdue.edu.

Notes

The authors declare no competing financial interest.
‖Shared first authorship.

■ ACKNOWLEDGMENTS

We thank Prof. G. Palmer and Dr. G. Soriano for helpful discussions and Dr. H. Böhme (ultimately Prof. Dr., Universität Bonn; deceased) for the initial (1971) observation of the split CD spectrum of the b_6f complex. These studies were supported by NIHGMS grant GM-038323 and the Henry Koffler Professorship (W.A.C.), the Division of Chemical Sciences, Geosciences, and Biosciences, Office of Basic Energy Sciences, Dept. of Energy, DEFG02-09ER1608 (S.S.), and a Purdue University Graduate Fellowship (S.S.H.).

■ REFERENCES

(1) Hosler, J. P.; Ferguson-Miller, S.; Mills, D. A. Energy transduction: Proton transfer through the respiratory complexes. *Annu. Rev. Biochem.* **2006**, *75*, 165−187.
(2) Nelson, N.; Yocum, C. F. Structure and function of photosystems i and ii. *Annu. Rev. Plant Biol.* **2006**, *57*, 521−565.
(3) Cramer, W. A.; Zhang, H.; Yan, J.; Kurisu, G.; Smith, J. L. Transmembrane traffic in the cytochrome b_6f complex. *Annu. Rev. Biochem.* **2006**, *75*, 769−790.
(4) Berry, E. A.; Guergova-Kuras, M.; Huang, L.-S.; Crofts, A. R. Structure and function of cytochrome *bc* complexes. *Annu. Rev. Biochem.* **2000**, *69*, 1005−1075.
(5) White, S. H. Biophysical dissection of membrane proteins. *Nature* **2009**, *459* (7245), 344−346.
(6) Solmaz, S. R.; Hunte, C. Structure of complex III with bound cytochrome *c* in reduced state and definition of a minimal core interface for electron transfer. *J. Biol. Chem.* **2008**, *283* (25), 17542−17549.
(7) Wenz, T.; Hielscher, R.; Hellwig, P.; Schagger, H.; Richers, S.; Hunte, C. Role of phospholipids in respiratory cytochrome bc_1 complex catalysis and supercomplex formation. *Biochim. Biophys. Acta* **2009**, *1787* (6), 609−616.
(8) Hasan, S. S.; Yamashita, E.; Cramer, W. A. Trans-membrane signaling and assembly of the cytochrome b_6f-lipidic charge transfer complex. *Biochim. Biophys. Acta* **2013**, *1827*, 1295−1308.
(9) Esser, L.; Elberry, M.; Zhou, F.; Yu, C. A.; Yu, L.; Xia, D. Inhibitor-complexed structures of the cytochrome bc_1 from the photosynthetic bacterium *Rhodobacter sphaeroides*. *J. Biol. Chem.* **2008**, *283* (5), 2846−2857.
(10) Hunte, C.; Richers, S. Lipids and membrane protein structures. *Curr. Opin. Struct. Biol.* **2008**, *18* (4), 406−411.
(11) Hasan, S. S.; Yamashita, E.; Baniulis, D.; Cramer, W. A. Quinone-dependent proton transfer pathways in the photosynthetic cytochrome b_6f complex. *Proc. Natl. Acad. Sci. U.S.A.* **2013**, *110*, 4297−4302.
(12) Kurisu, G.; Zhang, H.; Smith, J. L.; Cramer, W. A. Structure of the cytochrome b_6f complex of oxygenic photosynthesis: Tuning the cavity. *Science* **2003**, *302*, 1009−1014.
(13) Yamashita, E.; Zhang, H.; Cramer, W. A. Structure of the cytochrome b_6f complex: Quinone analogue inhibitors as ligands of heme c_n. *J. Mol. Biol.* **2007**, *370*, 39−52.
(14) Cerda, J. F.; Malloy, M. C.; Werkheiser, B. O.; Stockhausen, A. T.; Gallagher, M. F.; Lawler, A. C. Evaluation of heme peripheral group interactions in extremely low dielctric constant media and their contributions to the heme reduction potential. *Inorg. Chem.* **2013**, *53*, 182−188.
(15) Gilson, M. K.; Honig, B. H. The dielectric constant of a folded protein. *Biopolymers* **1986**, *25* (11), 2097−2119.
(16) Warshel, A.; Dryga, A. Simulating electrostatic energies in proteins: Perspectives and some recent studies of pka's, redox, and other crucial functional properies. *Proteins* **2011**, 3469−3484.
(17) Kallas, T. Cytochrome b_6f complex at the heart of energy transduction and redox signaling. *Adv. Photosynth. Respir.* **2012**, *34*, 501−560.

(18) Hauska, G.; Hurt, E.; Gabellini, N.; Lockau, W. Comparative aspects of quinol-cytochrome *c*/plastocyanin oxidoreductases. *Biochim. Biophys. Acta* **1983**, *726*, 97−133.
(19) Alric, J.; Pierre, Y.; Picot, D.; Lavergne, J.; Rappaport, F. Spectral and redox characterization of the heme c_i of the cytochrome b_6f complex. *Proc. Natl. Acad. Sci. U.S.A.* **2005**, *102* (44), 15860−15865.
(20) Pierre, Y.; Breyton, C.; Kramer, D.; Popot, J. L. Purification and characterization of the cytochrome b_6f complex from *Chlamydomonas reinhardtii*. *J. Biol. Chem.* **1995**, *270*, 29342−29349.
(21) Cramer, W. A.; Hasan, S. S.; Yamashita, E. The Q-cycle of cytochrome *bc* complexes: A structure perspective. *Biochim. Biophys. Acta* **2011**, *1807* (7), 788−802.
(22) Baniulis, D.; Yamashita, E.; Whitelegge, J. P.; Zatsman, A. I.; Hendrich, M. P.; Hasan, S. S.; Ryan, C. M.; Cramer, W. A. Structure-function, stability, and chemical modification of the cyanobacterial cytochrome b_6f complex from *Nostoc* sp. PCC 7120. *J. Biol. Chem.* **2009**, *284* (15), 9861−9869.
(23) Yan, J.; Kurisu, G.; Cramer, W. A. Intraprotein transfer of the quinone analogue inhibitor 2,5-dibromo-3-methyl-6-isopropyl-p-benzoquinone in the cytochrome b_6f complex. *Proc. Natl. Acad. Sci. U.S.A.* **2006**, *103* (1), 69−74.
(24) Stroebel, D.; Choquet, Y.; Popot, J.-L.; Picot, D. An atypical heam in the cytochrome b_6f complex. *Nature* **2003**, *426*, 413−418.
(25) Hunte, C.; Koepke, J.; Lange, C.; Rossmanith, T.; Michel, H. Structure at 2.3 Å resolution of the cytochrome bc_1 complex from the yeast saccharomyces cerevisiae co-crystallized with an antibody Fv fragment. *Structure* **2000**, *8* (6), 669−684.
(26) Iwata, S.; Lee, J. W.; Okada, K.; Lee, J. K.; Iwata, M.; Rasmussen, B.; Link, T. A.; Ramaswamy, S.; Jap, B. K. Complete structure of the 11-subunit bovine mitochondrial cytochrome bc_1 complex. *Science* **1998**, *281* (5373), 64−71.
(27) Zhang, Z.; Huang, L.; Shulmeister, V. M.; Chi, Y. I.; Kim, K. K.; Hung, L. W.; Crofts, A. R.; Berry, E. A.; Kim, S. H. Electron transfer by domain movement in cytochrome bc_1. *Nature* **1998**, *392*, 677−684.
(28) Widger, W. R.; Cramer, W. A.; Herrmann, R. G.; Trebst, A. Sequence homology and structural similarity between the *b* cytochrome of mitochondrial complex III and the chloroplast b_6f complex: Position of the cytochrome *b* hemes in the membrane. *Proc. Natl. Acad. Sci. U.S.A.* **1984**, *81*, 674−678.
(29) Zatsman, A. I.; Zhang, H.; Gunderson, W. A.; Cramer, W. A.; Hendrich, M. P. Heme-heme interactions in the cytochrome b_6f complex: EPR spectroscopy and correlation with structure. *J. Am. Chem. Soc.* **2006**, *128*, 14246−14247.
(30) Baymann, F.; Giusti, F.; Picot, D.; Nitschke, W. The c_i/b_H moiety in the b_6f complex studied by EPR: A pair of strongly interacting hemes. *Proc. Natl. Acad. Sci. U.S.A.* **2007**, *104* (2), 519−524.
(31) Bendall, D. S. *Protein electron transfer*; BIOS Scientific Publishers Limited: Oxford, U.K., 1996; p 304.
(32) Beratan, D.; Skourtis, S. Electron transfer mechanisms. *Curr. Opin. Chem. Biol.* **1998**, *2* (2), 235−243.
(33) Chamorovsky, S. K.; Cherepanov, D. A.; Chamorovsky, C. S.; Semenov, A. Y. Correlation of electron transfer rate in photosynthetic reaction centers with intraprotein dielectric properties. *Biochim. Biophys. Acta* **2007**, *1767* (6), 441−448.
(34) Gray, H. B.; Winkler, J. R. Electron transfer in proteins. *Annu. Rev. Biochem.* **1996**, *65*, 537−562.
(35) Moser, C. C.; Keske, J. M.; Warncke, K.; Farid, R. S.; Dutton, P. L. Nature of biological electron transfer. *Nature* **1992**, *355* (6363), 796−802.
(36) Castellani, R.; Covian, R.; Kleinschroth, T.; Anderka, O.; Ludwig, B.; Trumpower, B. L. Direct demonstration of half-of-the-sites reactivity in the dimeric cytochrome bc_1 complex. *J. Biol. Chem.* **2010**, *285*, 507−510.
(37) Covian, R.; Trumpower, B. L. Regulatory interactions in the dimeric cytochrome bc_1 complex: The advantages of being a twin. *Biochim. Biophys. Acta* **2008**, *1777* (9), 1079−10791.
(38) Crofts, A. R.; Holland, J. T.; Victoria, D.; Kolling, D. R.; Dikanov, S. A.; Gilbreth, R.; Lhee, S.; Kuras, R.; Kuras, M. G. The Q-cycle reviewed: How well does a monomeric mechanism of the bc_1 complex account for the function of a dimeric complex? *Biochim. Biophys. Acta* **2008**, *1777* (7−8), 1001−1019.
(39) Czapla, M.; Borek, A.; Sarewicz, M.; Osyczka, A. Enzymatic activities of isolated cytochrome bc_1-like complexes containing fused cytochrome *b* subunits with asymmetrically inactivated segments of electron transfer chains. *Biochemistry* **2012**, *51* (4), 829−835.
(40) Khalfaoui-Hassani, B.; Lanciano, P.; Lee, D. W.; Darrouzet, E.; Daldal, F. Recent advances in cytochrome bc_1: Inter monomer electronic communication? *FEBS Lett.* **2012**, *586* (5), 617−621.
(41) Lanciano, P.; Lee, D. W.; Yang, H.; Darrouzet, E.; Daldal, F. Intermonomer electron transfer between the low-potential *b* hemes of cytochrome *bc*. *Biochemistry* **2011**, *50* (10), 1651−1663.
(42) Shinkarev, V. P.; Wraight, C. A. Intermonomer electron transfer in the bc_1 complex dimer is controlled by the energized state and by impaired electron transfer between low and high potential hemes. *FEBS Lett.* **2007**, *581* (8), 1535−1541.
(43) Swierczek, M.; Cieluch, E.; Sarewicz, M.; Borek, A.; Moser, C. C.; Dutton, P. L.; Osyczka, A. An electronic bus bar lies in the core of cytochrome bc_1. *Science* **2010**, *329* (5990), 451−454.
(44) Gutierrez-Cirlos, E. B.; Trumpower, B. L. Inhibitory analogs of ubiquinol act anti-cooperatively on the yeast cytochrome bc_1 complex. *J. Biol. Chem.* **2002**, *277* (2), 1195−1202.
(45) Hunte, C.; Solmaz, S.; Palsdottir, H.; Wenz, T. A structural perspective on mechanism and function of the cytochrome bc_1 complex. *Results Probl. Cell Differ.* **2008**, *45*, 253−278.
(46) Xia, D.; Esser, L.; Elberry, M.; Zhou, F.; Yu, L.; Yu, C. A. The road to the crystal structure of the cytochrome bc_1 complex from the anoxygenic, photosynthetic bacterium *Rhodobacter sphaeroides*. *J. Bioenerg. Biomembr.* **2008**, *40* (5), 485−492.
(47) Czapla, M.; Borek, A.; Sarewicz, M.; Osyczka, A. Fusing two cytochromes *b* of *Rhodobacter capsulatus* cytochrome bc_1 using various linkers defines a set of protein templates for asymmetric mutagenesis. *Protein Eng., Des. Sel.* **2012**, *25* (1), 15−25.
(48) Soriano, G. M.; Ponamarev, M. V.; Carrell, C. J.; Xia, D.; Smith, J. L.; Cramer, W. A. Comparison of the cytochrome bc_1 complex with the anticipated structure of the cytochrome b_6f complex: Le plus ca change le plus c'est la meme chose. *J. Bioenerg. Biomembr.* **1999**, *31* (3), 201−213.
(49) Gong, X.; Yu, L.; Xia, D.; Yu, C. A. Evidence for electron equilibrium between the two hemes bl in the dimeric cytochrome bc_1 complex. *J. Biol. Chem.* **2005**, *280* (10), 9251−9257.
(50) Joliot, P.; Joliot, A. The low-potential electron-transfer chain in the cytochrome *bf* complex. *Biochim. Biophys. Acta* **1988**, *933*, 319−333.
(51) Palmer, G.; Degli Esposti, M. Application of exciton coupling theory to the structure of mitochondrial cytochrome *b*. *Biochemistry* **1994**, *33* (1), 176−185.
(52) Schoepp, B.; Chabaud, E.; Breyton, C.; Vermeglio, A.; Popot, J.-L. On the spatial organization of hemes and chlorophyll in cytochrome b_6f. *J. Biol. Chem.* **2000**, *275*, 5275−5283.
(53) Hurt, E. C.; Hauska, G. Cytochrome-b_6f from isolated cytochrome- b_6f complexes - evidence for 2 spectral forms with different midpoint potentials. *FEBS Lett.* **1983**, *153* (2), 413−419.
(54) Rich, P. R.; Madgwick, S. A.; Moss, D. A. The interactions of duroquinol, DBMIB, and nqno with the chloroplast cytochrome *bf* complex. *Biochim. Biophys. Acta* **1991**, *1058*, 312−328.
(55) Furbacher, P. N.; Girvin, M. E.; Cramer, W. A. On the question of interheme electron transfer in the chloroplast cytochrome b_6 *in situ*. *Biochemistry* **1989**, *28*, 8990−8998.
(56) Girvin, M. E.; Cramer, W. A. A redox study of the electron transport pathway responsible for generation of the slow electrochromic phase in chloroplasts. *Biochim. Biophys. Acta* **1984**, *767*, 29−38.
(57) Baniulis, D.; Hasan, S. S.; Stofleth, J. T.; Cramer, W. A. Mechanism of enhanced superoxide production in the cytochrome b_6f complex of oxygenic photosynthesis. *Biochemistry* **2013**, *52*, 8975−8983.

(58) Baniulis, D.; Zhang, H.; Yamashita, E.; Zakharova, T.; Hasan, S. S.; Cramer, W. A. Purification and crystallization of the cyanobacterial cytochrome b_6f complex. *Methods in Molecular Biology, Photosynthesis Research Protocols*; Carpentier, R., Ed.; Humana Press Inc: Totowa, NJ, 2011; pp 65−77.
(59) Zhang, H.; Whitelegge, J. P.; Cramer, W. A. Ferredoxin:NADP$^+$ oxidoreductase is a subunit of the chloroplast cytochrome b_6f complex. *J. Biol. Chem.* **2001**, *276*, 38159−38165.
(60) Mayhew, S. G. The redox potential of dithionite and SO^-_2 from equilibrium reactions with flavodoxins, methyl viologen and hydrogen plus hydrogenase. *Eur. J. Biochem.* **1978**, *85* (2), 535−547.
(61) Metzger, S. U.; Cramer, W. A.; Whitmarsh, J. Critical analysis of the extinction coefficient of chloroplast cytochrome *f*. *Biochim. Biophys. Acta* **1997**, *1319*, 233−241.
(62) Degli Esposti, M.; Crimi, M.; Samworth, C. M.; Solaini, G.; Lenaz, G. Resolution of the circular dichroism spectra of the mitochondrial cytochrome bc_1 complex. *Biochim. Biophys. Acta* **1987**, *892* (3), 245−252.
(63) Degli Esposti, M.; Palmer, G.; Lenaz, G. Circular dichroic spectroscopy of membrane haemoproteins. The molecular determinants of the dichroic properties of the *b* cytochromes in various ubiquinol:Cytochrome *c* reductases. *Eur. J. Biochem.* **1989**, *182* (1), 27−36.
(64) Van Amerongen, H.; Valkunas, L.; Van Grondelle, R. *Photosynthetic excitons*; World Scientific: Singapore, 2000; Chapters 2 and 3.
(65) Wenk, S.-O.; Schneider, D.; Boronowsky, U.; Jager, C.; Klughammer, C.; de Weerd, F. L.; van Roon, H.; Vermaas, W. F. J.; Dekker, J. P.; Raegner, M. Functional implications of pigments bound to a cyanobacterial cytochrome b_6f complex. *FEBS Lett.* **2005**, *272*, 582−592.
(66) Lambeth, D. O.; Palmer, G. The kinetics and mechanism of reduction of electron transfer proteins and other compounds of biological interest by dithionite. *J. Biol. Chem.* **1973**, *248* (17), 6095−6103.
(67) Warshel, A.; Aqvist, J. Electrostatic energy and macromolecular function. *Annu. Rev. Biophys. Biophys. Chem.* **1991**, *20*, 267−298.
(68) Alexov, E. G.; Gunner, M. R. Calculated protein and proton motions coupled to electron transfer: Electron transfer from Q_A- to Q_B in bacterial photosynthetic reaction centers. *Biochemistry* **1999**, *38* (26), 8253−8270.
(69) Miyashita, O.; Onuchic, J. N.; Okamura, M. Y. Continuum electrostatic model for the binding of cytochrome c2 to the photosynthetic reaction center from *Rhodobacter sphaeroides*. *Biochemistry* **2003**, *42* (40), 11651−11660.
(70) Steffen, M. A.; Lao, K.; Boxer, S. G. Dielectric asymmetry in the photosynthetic reaction center. *Science* **1994**, *264* (5160), 810−816.
(71) Dashdorj, N.; Xu, W.; Martinsson, P.; Chitnis, P. R.; Savikhin, S. Electrochromic shift of chlorophyll absorption in photosystem I from *Synechocystis* sp. PCC 6803: A probe of optical and dielectric properties around the secondary electron acceptor. *Biophys. J.* **2004**, *86* (5), 3121−3130.
(72) Kramer, D. M.; Crofts, A. R. Re-examination of the properties and function of the *b* cytochromes of the thylakoid cytochrome *bf* complex. *Biochim. Biophys. Acta* **1994**, *1184*, 193−201.
(73) Girvin, M. E. Electron and proton transfer in the quinone-cytochrome *bf* region of chloroplasts. Ph.D. Thesis, Purdue University, 1985.
(74) Krishtalik, L. I. Role of the protein's low dielectric constant in the functioning of the photosynthetic reaction center. *Photosynth. Res.* **1999**, *60*, 241−246.
(75) Marcus, R. A. On the theory of electron transfer reactions. Vi. Unified treatment for homogeneous and electrode reactions. *J. Chem. Phys.* **1965**, *43*, 679−701.
(76) Marcus, R. A.; Sutin, N. Electron transfers in chemistry and biology. *Biochim. Biophys. Acta* **1984**, *811*, 265−322.
(77) Hasan, S. S.; Yamashita, E.; Ryan, C. M.; Whitelegge, J. P.; Cramer, W. A. Conservation of lipid functions in cytochrome *bc* complexes. *J. Mol. Biol.* **2011**, *414* (1), 145−162.
(78) Crofts, A. R.; Guergova-Kuras, M.; Kuras, R.; Ugulava, N.; Li, J. Y.; Hong, S. J. Proton-coupled electron transfer at the Q_o site: What type of mechanism can account for the high activation barrier? *Biochim. Biophys. Acta, Bioenerg.* **2000**, *1459* (2−3), 456−466.
(79) Hasan, S. S.; Cramer, W. A. On rate limitations of electron transfer in the photosynthetic cytochrome b_6f complex. *Phys. Chem. Chem. Phys.* **2012**, *14*, 13853−13860.
(80) Hasan, S. S.; Cramer, W. A. Internal lipid architecture of the hetero-oligomeric cytochrome b_6f complex. *Structure* **2014**, in press DOI: 10.1016/j.str.2014.05.004.

NOTE ADDED IN PROOF

During the revision of the current manuscript, a 2.5 Å electron density map of the cytochrome b_6f complex (PDB ID 4OGQ) has been published, which shows an extensive lipid component within the inter-monomer cavity.[80]